Electrochimica Acta 136 (2014) 112–120

Contents lists available at ScienceDirect

Electrochimica Acta

journal homepage: www.elsevier.com/locate/electacta

Effect of binder properties on electrochemical performance for silicon-graphite anode: Method and application of binder screening

Taeeun Yim [a], Soo Jung Choi [a], Yong Nam Jo [a], Tae-Hyun Kim [b], Ki Jae Kim [a], Goojin Jeong [a], Young-Jun Kim [a,*]

[a] Advanced Batteries Research Center, Korea Electronics Technology Institute, 68 Yatap-dong, Bundang-gu, Seongnam, Gyeonggi-do 463-816, Republic of Korea
[b] Department of Chemistry, Incheon National University, Academy-ro 119, Songdo-dong, Yeonsu-gu, Incheon, 460-772, Republic of Korea

ARTICLE INFO

Article history:
Received 3 March 2014
Received in revised form 15 April 2014
Accepted 12 May 2014
Available online 27 May 2014

Keywords:
Lithium ion battery
Binder
Silicon anode
Poly(acrylic acid)
Poly(amide imide)

ABSTRACT

With increasing demand for lithium-ion batteries (LIBs) with high energy density, silicon-based negative electrode material has attracted much interest because of its high specific capacity. Practical utilization of Si remains unattainable, however, owing to severe volume expansion in the electrode, resulting in a loss of the electrical Si network, which is directly connected to drastic capacity fading of the cell. Therefore, there have been systematic studies on the characterization of fundamental binder properties to estimate the suitability of various binder materials. The binder properties are subdivided into mechanical and adhesion characteristics, electrode properties (rigidity and recovery), and phase separation behavior of slurry to correlate with the electrochemical performance and practical acceptance of candidate materials. Systematic screening showed that hybridization of poly(acrylic acid) (PAA) and poly(amide imide) (PAI) could complement each other's properties and the hybridized PAA–PAI was synthesized by a one-step, acid-catalyzed reaction. The PAA–PAI hybrid showed enhancement in overall properties as a result of co-polymerization and exhibited remarkable cycling performance after 300 cycles. Based on these results, it can be concluded that an understanding of binder characteristics provides useful insight into the search for a more efficient binder material, and fine tuning of fundamental binder properties through screening will be advantageous to the construction of more efficient LIB systems

1. Introduction

Lithium-ion batteries (LIBs) are the most attractive energy-storage systems based on their moderate rate capability, long cycle life, and high gravimetric and volumetric energy density [1–3]. As the demand for large-scale LIBs increases, they have emerged as promising power sources for hybrid-electric vehicles (HEVs), electric vehicles (EVs), and energy-storage systems (ESS) [4–8]. The relatively low energy density of currently available LIBs, however, presents a significant obstacle to their more widespread adoption, and much higher energy densities are needed for many practical applications. In this regard, silicon is one of the prospective anode materials owing to its excellent specific capacity (4200 mAh g^{-1}), which exceeds that of a conventional graphite anode (360 mAh g^{-1}) by an order of magnitude [9–11]. However, practical utilization of Si remains a challenge as the continuous irreversible electrochemical reaction of Si readily leads to poor cycling performance. This drawback mainly results from the intrinsic electrochemical nature of Si, where the electrochemical conversion of Si to Li_xSi_y is always accompanied by severe volume expansion in the electrode, causing it to pulverize and leading to isolation of the active material [12–14]. With the loss of an electrical network, the electrode is unable to process further electrochemical reaction, resulting in drastic capacity fading in cycling performance. Therefore, effective control of volume changes is the most indispensable requirement for utilization of Si. In this respect, an understanding of binder properties is essential as the primary role of the binder is to enhance the binding affinity between solid components (active material, carbon conductor) and the current collector in order to maintain an electronic network with a certain level of electrode uniformity to facilitate electrochemical reaction. Hence, many new candidate binder materials have been intensively investigated to promote binding interaction with the surfaces of Si particles or to facilitate Li^+ ion migration [15–20]; however, the operating principle

* Corresponding author.
E-mail address: yjkim@keti.re.kr (Y.-J. Kim).

http://dx.doi.org/10.1016/j.electacta.2014.05.062
0013-4686/

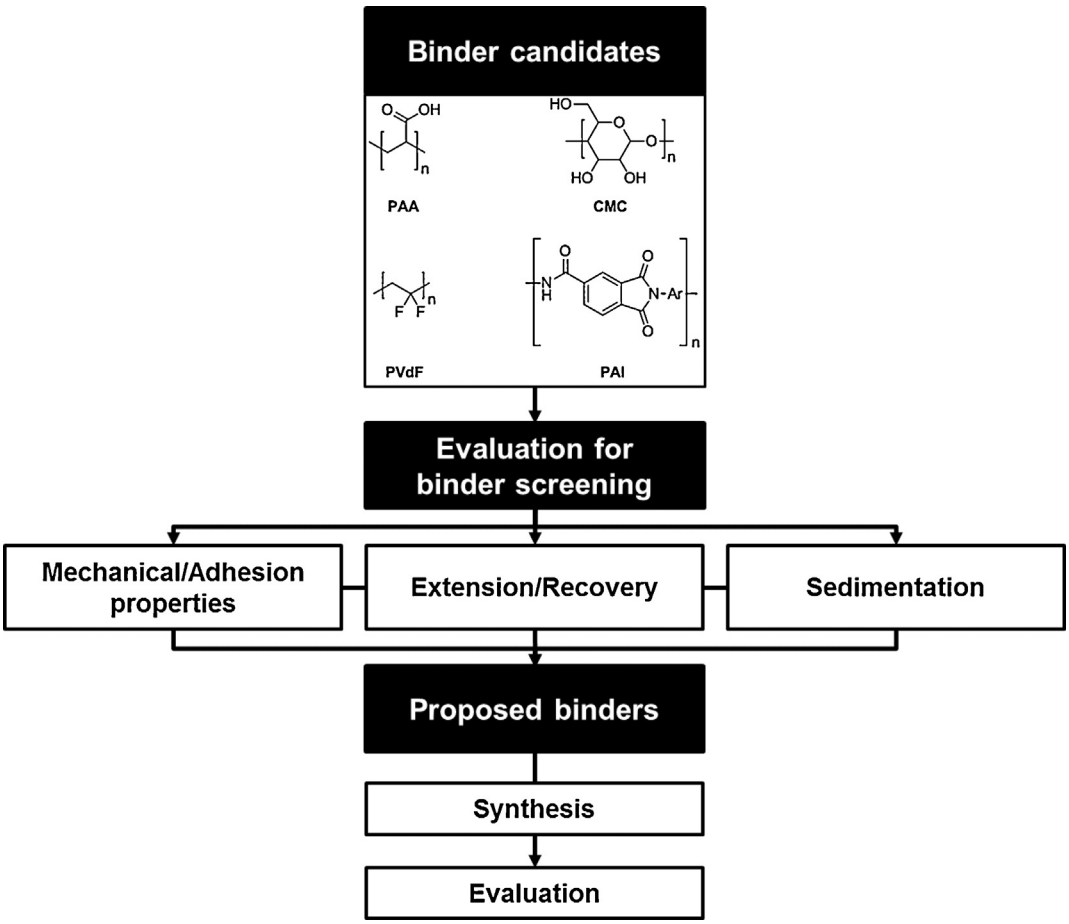

Fig. 1. Chemical structure of binder candidates and systematic strategy for binder screening method based on evaluation their properties.

of binders, namely, the main factor that enhances cycling performance, remains unclear. It has been observed that a binder with enhanced mechanical properties can help suppress volume expansion; however, its successful application is not assured because other factors including adhesion and slurry and electrode properties obviously affect the electrochemical performance as well. Therefore, a comprehensive assessment of the combination of binder properties with electrode properties is a useful and necessary probing tool to evaluate binder candidates. In this work, a systematic procedure for characterization of binder properties was established in terms of binding affinity, and the degree of extension and recovery in the electrode; it also included an analysis of phase separation behavior of slurries depending on the binder material (Fig. 1). The binding affinity is categorized according to the binding mechanism: i) mechanical properties of binders; ii) adhesion between the binder and Cu current collector. Insight into the effect of binding affinity on electrode performance will be useful in identifying the dominant factor of binder performance to maintain a desirable electrode network. As the factor of phase separation properties significantly affects electrode uniformity, which determines cell performance, an understanding of the phase separation behavior of various binders will be helpful to determine the processability of the material in industrial settings. Based on these assessments, promising binder materials were screened from candidates including (poly(acrylic acid) (PAA), carboxymethyl cellulose (CMC), poly(vinylidine difluoride) (PVdF), and poly(amide imide) (PAI)). A new hybridized binder was then synthesized, through which the complementary properties of individual materials were combined to form improved properties.

2. Experimental

2.1. Measurement of mechanical and adhesion properties

To measure the mechanical properties of the binders, 5 g of each binder was dissolved in 10 mL of solvent (water for PAA (Aldrich, average MW: 100,000) and CMC (Aldrich, average MW: 90,000); *N*-methyl-2-pyrrolidone (NMP) for PVdF (Kureha, KF1100, average MW: 280,000) and PAI (Solvay, Torlon 4000T) to prepare the binder solution. After completion of binder dissolution, they were casted on Teflon (in case of water-based solution) or a glass mold (in case of NMP-based solution), respectively, and then dried in a vacuum oven overnight. The specimens were cut to pieces with the same dimensions (10 cm (width) × 30 cm (length) × 100 μm (thickness)) and their mechanical properties were measured by a tensile strength tester (JSV-H1000, Coretech).

To evaluate adhesion properties of binder, a mixture of the active material (silicon:graphite = 3:7), binder, and carbon conductor (Super P) (in a weight ratio of 8:1:1) was dispersed in the solvent (water or NMP). The slurry formed from the dispersion was coated on a piece of copper foil, and the resulting electrode was dried in a vacuum oven at 120 °C for 12 h. After drying was completed, the electrode was completely attached onto slide glass with the identical dimensions (10 cm (width) × 30 cm (length) × 100 μm (thickness)) using a double-sided adhesive tape. Their adhesion properties were measured by a tensile strength tester (JSV-H1000, Coretech). Because delamination is only arisen between coating layer and Cu-current collector, recording stress measured in a tensile strength tester is considered as adhesive force.

2.2. Evaluation of electrode indentation

To measure the rigidity and recovery of different binder materials, all electrode specimens were cut to identical dimensions (1 cm × 1 cm). Each specimen was subjected to an indentation test using a microindentor (DUH-211, Shimadzu). The probe of the microindentor was placed on top of the electrode surface and the depth of the pressed electrode was recorded as a function of the external force. After the external force reached 10 mN, the electrode recovery was recorded as the external force was removed, and the rigidity and recovery ratio was analyzed by calculating the changes in the indentation depth profile.

2.3. Characterization of degree of phase separation in slurries

First, 10 g of binder was dissolved in 100 mL of each solvent (water or NMP). Next, other solid components (80 g of active material (silicon:graphite = 3:7) and 10 g of carbon conductor (Super P)) were added to the solution and finely dispersed by a mechanical stirrer (Primix) for 3 h. After mixing was completed, each slurry was kept in a 100-mL mess cylinder for 7 days at room temperature. The separated layers were then collected and dried in a 100 °C oven overnight. Finally, the degree of phase separation was calculated by the ratio of changes in the weight of the solid components.

2.4. Synthesis of PAA-PAI and characterization of their chemical structure

For the synthesis of PAA–PAI, 5 g of PAA was dissolved in 70 mL of water until it formed a homogeneous solution. After 0.05 g of sulfuric acid (1 wt.%) and 5 g of PAI were added to the solution, the reaction temperature was increased to 100 °C for 24 h. The supernatant was then filtered to remove any precipitated PAI, which was the undissolved raw material, and the remaining solvent was evaporated under reduced pressure at 100 °C for 12 h. The remaining solid was re-dissolved in a minimal amount of water, which was subsequently evaporated under vacuum at 150 °C for 12 h. The remaining solid was washed with diethyl ether and ethyl acetate several times to remove any organic impurities and was then dried in a vacuum oven overnight. The chemical structure of the product was characterized by an FT-IR spectrometer (VERTEX 70, Bruker) in the attenuated total reflection (ATR) mode under a N_2 atmosphere and a ^{13}C-NMR spectrometer (ASCEND^{TM} 400, Bruker).

2.5. Evaluation of cycle performance

A mixture of the active material (silicon (50 nm, round-type, Alfa Aesar):graphite (17 μm, round-type, Poscochemtech, Korea) = 3:7), binder, and carbon conductor (Super P) (in a weight ratio of 8:1:1) was dispersed in the solvent (water or NMP). The slurry formed from the dispersion was coated on a piece of copper foil, and the resulting electrode plate was dried in a vacuum oven at 120 °C for 12 h. The loading and electrode densities were fixed at 1.50 mg cm^{-2} and 1.00 g cm^{-3}, respectively. Galvanostatic discharge–charge cycling was performed using a beaker-type three-electrode cell, which was assembled using the anode, lithium foil, poly(ethylene) separator, and electrolyte (mixture of ethylene carbonate (EC) and ethylmethylcarbonate (EMC) in a ratio of EC:EMC = 1:2 with 1 M $LiPF_6$ and 10 wt.% fluoro-ethylene carbonate (FEC); PanaxEtec). The cell was assembled in a dry room, where the dew point was below -60 °C. It was galvanostatically discharged to 0.01 V vs. Li/Li$^+$ and charged to 1.5 V vs. Li/Li$^+$ repeatedly at a constant C-rate of 5 C at room temperature using a battery cycler (TOSCAT-3100, Toyo). Half-cells were fabricated using different binders and were galvanostatically charged and discharged at 0.1 C rate to measure the volume expansion of the electrode materials. The cycled half-cells were dismantled in an Ar-filled glove box and were then cross-sectioned using a cross-section polisher (CP, JEOL/sn-09010). Field emission scanning electron microscopy (FE-SEM, JEOL JSM-7000F) was used to measure the electrode heights.

3. Result and discussion

3.1. Mechanical and adhesion properties of binders

It is well recognized that the mechanical property is a major parameter that determines cycling performance of a Si anode because better mechanical property is more beneficial to maintenance of a consistent electrically conducting network, leading to suppression of electrochemical grinding of solid-contents in electrode during the electrochemical process [21,22]. In this respect, stress–strain curves of only binder films provide useful information to evaluate their mechanical properties because they offer clues on ultimate strength, Young's modulus, etc. The mechanical properties of the binder materials examined here were investigated by measuring the stress–strain curves of films casted from each binder material (Fig. 2a). Results of the mechanical properties (measured for binder films only) showed that PAA was the most effective binder: it displayed the largest stress at break (ultimate tensile strength, 32.8 MPa) and the highest Young's modulus (7.95 MPa); it also showed a relatively large extension prior to breaking. These results suggest that a PAA binder, with high stiffness and moderate elastomeric properties, will be stable and will resist both elastic and plastic deformations during the volume changes of the Si anode. By contrast, other binder candidates exhibited lower stiffness than PAA and had lower Young's moduli; among them, PVdF displayed a much lower stiffness value and Young's modulus than CMC and PAI. These results suggest that once PVdF was deformed, it would be largely incapable of maintaining contact with the Si particles during their subsequent contraction, which could explain its reportedly poor performance in Si anodes [18,23,24].

The adhesion strength (an attractive force in the interaction between the binder and Cu current collector) is another important factor that can assure better performance of the cell. Because delamination of active Si from the current collector can significantly increase capacity fading as a result of the increase in internal resistance [25,26], high adhesive force is required to maintain the electronic network of the electrode. The results from the adhesion test (measuring the stress that appeared in the delamination of active material from the Cu current collector), however, showed quite different behavior compared to that in the mechanical property test (Fig. 2b): the most desirable adhesion behavior was observed in PAI instead of PAA which had excellent mechanical properties. PAI exhibited relatively larger stress at break in accordance with electrode delamination (3.14 mN mm^{-1}). This means that PAI was more effective in suppressing delamination of active species from the Cu current collector, and the electrical contact in the electrode remained uniform. This analysis suggests that PAA and PAI are suitable materials for the Si anode based on their better binding affinity. An understanding of the correlation between binding mechanism and cycling performance would be helpful to explain why the mechanical and adhesion properties are important for the performance of a Si anode.

3.2. Effect of binding affinity on extension and recovery in electrode

To analyze the effect of binding affinity on changes in the electrode and estimate the binder performance, the indentation tester was adopted as a simulation tool. Ideally, both rigid and elastic characteristics are required for the binder in a Si–graphite anode

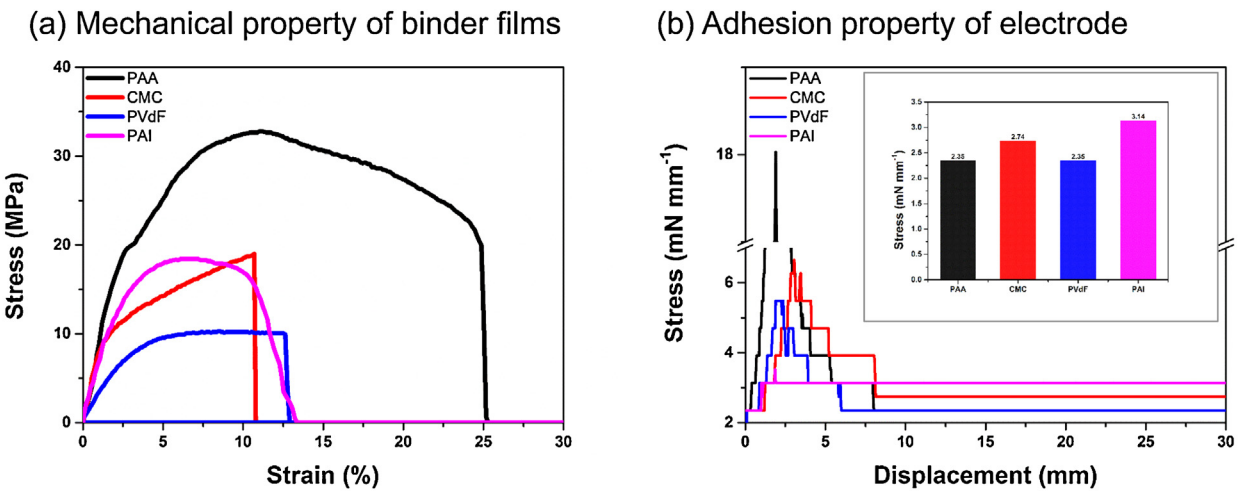

Fig. 2. (a) Stress-strain curves for characterization of mechanical property of binder film depending on binders, (b) Adhesion property of electrode depending on binder.

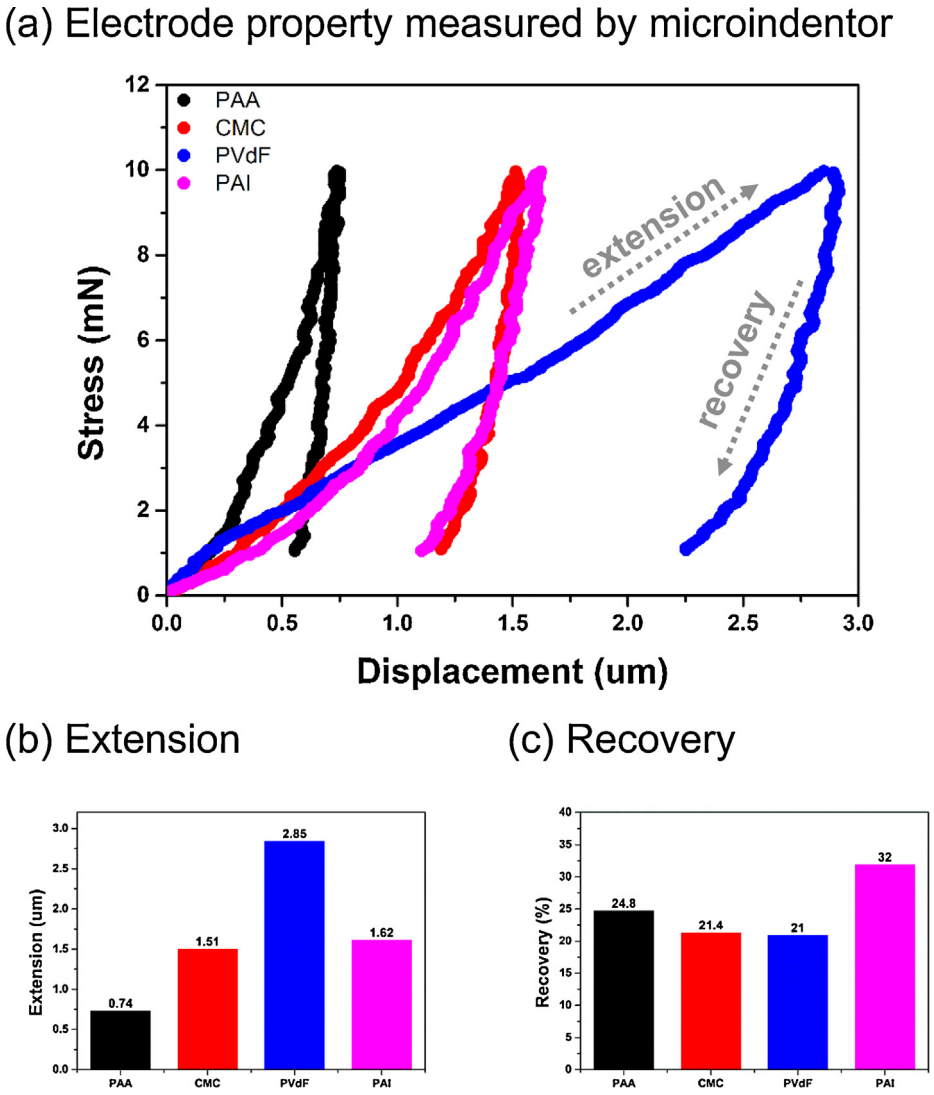

Fig. 3. (a) Indentation results of electrode measured by microindentor, (b) Degree of extension in electrode depending on binder candidates, (c) Degree of recovery in electrode depending on binder candidates.

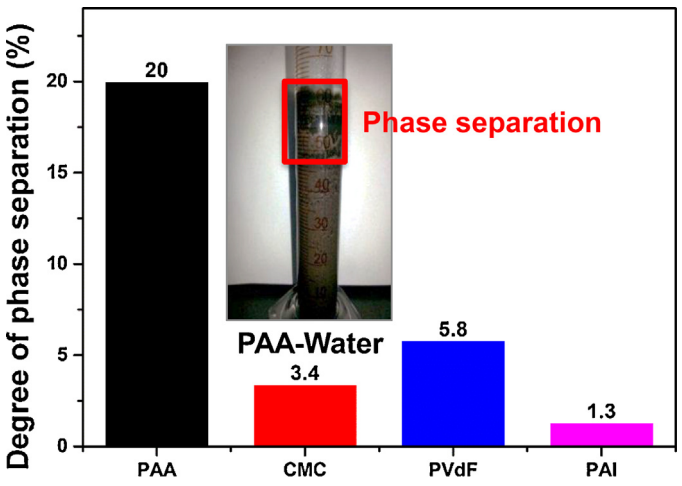

Fig. 4. Analysis results for degree of phase separation behavior in slurry depending on binder candidates.

because rigidity (lower degree of extension during displacement) can prevent electrochemical grinding of Si and elasticity (higher recovery after displacement) can help retain electrical contact during electrode contraction in de-lithiation of Si. In this respect, it is useful to examine the indentation because changes in thickness resulting from deformation and the recovery of the electrode provide informative clues on binder performance, as shown by the measurement results in Fig. 3. The degree of extension in the electrode was highly influenced by the mechanical property of the binder candidate. PAA, which had an excellent ultimate tensile strength, exhibited the lowest degree of extension. Both PAI and CMC, which had moderate ultimate tensile strength, showed relatively larger extensions than PAA; however, they were still quite effective in suppressing electrode deformation when compared to PVdF, which had poor mechanical properties. This means that the mechanical property is a crucial factor that determines the permanent transformations in the electrode and PAA was the most attractive candidate based on the lower deformation incurred owing to its excellent rigidity. On the contrary, electrode recovery appeared to be irrelevant to the mechanical properties: the highest recovery was observed in PAI (32.0%), which is a relatively soft material based on its low Young's modulus, while other binder candidates with higher Young's moduli (PAA and CMC) showed lower recovery (24.8% and 21.4%, respectively) than PAI. This indicates that PAI was the most promising candidate for maintaining the electrical conducting network of the electrode because of its excellent elasticity. Therefore, it can be concluded that PAA and PAI are highly desirable materials for the Si–graphite anode based on their remarkable rigidity and elasticity, respectively.

3.3. Analysis for phase separation of various binders

Although the phase separation behavior of a slurry does not significantly affect the electrochemical performance of the electrode on a laboratory scale, it has considerable effect on the electrode uniformity on an industrial scale, as manifested in properties such as distribution in loading and electrode density which are one of important factor to determine their practical availability. The phase separation behavior can be assessed by a simple storage test of the slurry: observation of phase separation followed by measurement of the weight of solid components of the precipitated or separated layer. PAA showed considerable phase separation after the storage test, which resulted in 20.0% of phase separation (Fig. 4). This indicates that even though PAA effectively controlled electrochemical grinding of Si based on its excellent mechanical strength and

Table 1
Analysis results for mechanical properties of binder film.

Binder	Ultimate strength (MPa)	Young's modulus (MPa)	Adhesion stress (mN mm $^{-1}$)
PAA	32.8	7.95	2.35
CMC	19.0	5.47	2.74
PVdF	10.1	1.62	2.35
PAI	18.4	4.90	3.14

rigidity, the large amount of phase separation did not allow it to gain practical acceptance owing to difficulty in obtaining quality assurance of the electrode. It is believed that the phase separation behavior of PAA is the main hindrance in commercialization of the binder despite numerous reports in the literature proving the positive effect of PAA on cycling performance. Otherwise, other binder candidates showed better slurry states after the storage test: the most effective binder candidate was PAI based on the lower degree of phase separation (1.3%). Even the commercialized binders (CMC and PVdF) exhibited higher phase separation behavior than PAI. The results indicate that the PAI is the most promising candidate in terms of processability, which is expected to yield better electrode uniformity.

3.4. Summary of basic binder properties

All of binder candidates showed unique characteristics owing to their different nature. PAA is the most likely to be adopted for application in Si–graphite electrodes because it showed excellent mechanical properties and the lowest electrode deformation owing to its outstanding rigidity. However, its relatively lower adhesion affinity and poor processability must be overcome in order to attain better cycle life along with practical acceptance. In this regard, PAI is an attractive alternative to PAA: although PAI has relatively inferior properties such as mechanical properties and extension compared to PAA, its remarkable adhesion affinity and phase separation behavior can adequately offset the poor properties of PAA in adhesion and phase separation behavior. In addition, the remaining excellent PAI electronic-conduction network was favorable for facilitating Li^+ ion migration in the electrode, thereby increasing the specific capacity of the Si-based anode [19,20]. Therefore, it is expected that fine tuning the fundamental properties via co-polymerization of PAA and PAI would be applicable to the Si–graphite anode.

Table 1

3.5. Synthesis and characterization of PAA-PAI

The synthesis scheme for PAA–PAI is shown in Fig. 5a. We used an acid catalyst to protonate the PAI so that it became water soluble and vacuum dehydration to accelerate the formation of the new amide functionality in the PAA-PAI because the reaction between carboxylic acids and imides requires high activation energy [27,28]. Spectroscopic analysis was used to show that the PAA-PAI had been synthesized: The FT-IR spectrum clearly showed an absorbance signal at 1713 cm^{-1}, associated with the (R–C(O)–N–R_2, R: alkyl or aryl) amide vibration, and the ^{13}C-NMR spectra showed a signal at 176.9 ppm, corresponding to the amide functional group (Figs. 5b and c) [29,30], in accordance with the remaining carboxylic groups in the PAA-PAI (i.e., the unreacted carboxylic acid might be from the sterically hindered PAA-PAI structure). These results suggest that the PAA-PAI was bifunctionalized; that is, it showed carboxylic functionalities (which could provide the anode composite with interaction sites) partially distributed on the main polymeric chains in accordance with the changes in the main PAA-PAI polymeric frame. Further investigation to evaluate the new binder's

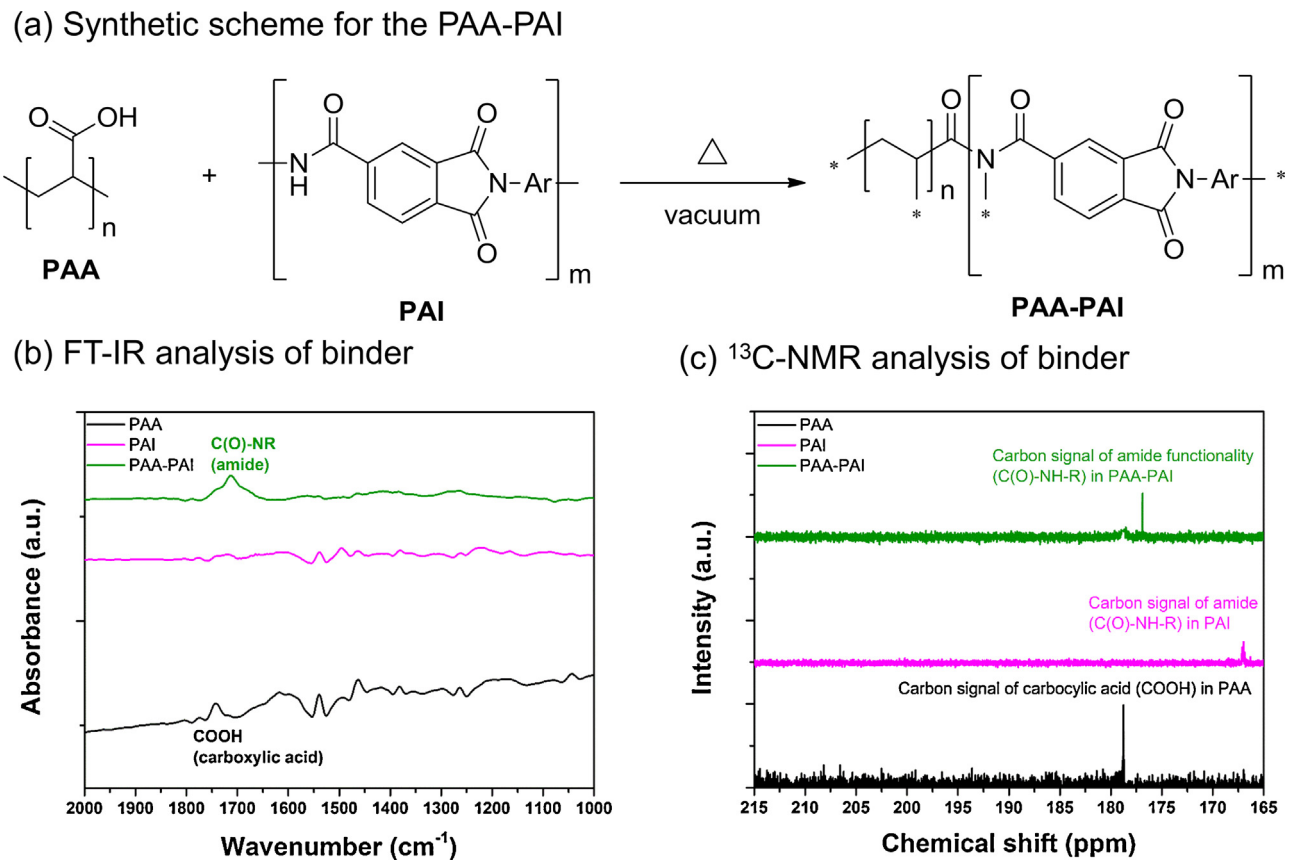

Fig. 5. (a) Synthetic scheme for the PAA-PAI, (b) FT-IR analysis results for the PAA (black), PAI (pink) and PAA-PAI (green), (c) ^{13}C-NMR spectroscopy for the PAA (black), PAI (pink) and PAA-PAI (green).

properties was attempted to compare the results with previous findings (Fig. 6 and Table 2). It was clearly observed that PAA–PAI showed well-balanced and enhanced binder properties as a result of hybridization. The relatively less mechanical property and rigidity in PAI and poor phase separation behavior in PAA were improved in PAA–PAI. It appeared that each disadvantage of PAA and PAI was reversed as a result of co-polymerization. Interestingly, the adhesion affinity and elasticity in PAA–PAI was much higher than PAI even though these parameters were considered weaknesses of PAA. It is not clear why these enhanced properties were observed in PAA–PAI, although it might be assumed that additional crosslinking reaction occurring in co-polymerization (intramolecular or intermolecular reaction) could further soften PAA–PAI, resulting in changes in the adhesive property and the hybrid's elasticity. Further studies on the effect of co-polymerization on binder properties are still ongoing in our laboratory.

3.6. Evaluation of electrochemical performance of PAA-PAI

To clarify the effect of enhanced binder properties on the electrochemical performance, the rate capability and cycling performance of PAA–PAI were evaluated and compared to the results for PAA and PAI. The most remarkable difference in electrochemical performance was observed in the practical utilization of the anode material: the cell consisting of PAA–PAI exhibited much better rate capability even at high rate (5 C) condition compared to the cells consisting of PAA and PAI (Fig. 7a). Much higher specific capacity was also observed in the cycling performance: the initial specific capacity of PAA–PAI was much higher than those of PAA and PAI (1120.9 mAh g^{-1} vs. 974.1 and 871.7 mAh g^{-1}, respectively) (Fig. 7b) in accordance with the improved coulombic efficiency (inset in Fig. 7b). In addition, the capacity retention of PAA–PAI at the end of 100 cycles was higher than those of PAA and PAI: the cell cycled with PAA–PAI showed 66.2% of the specific capacity remaining after 100 cycles (742.4 mAh g^{-1}), compared to the cells cycled with PAA and PAI, which exhibited 61.4% and 60.9% retentions, respectively (with corresponding specific capacities of 598.2 and 530.8 mAh g^{-1} after 100 cycles). At the end of 300 cycles, the cell with PAA–PAI showed excellent retention based on the higher remaining specific capacity (47.0%, 527.1 mAh g^{-1}) compared to the cells with PAA and PAI, which showed much lower retention as a result of severe capacity fading (38.2%,

Table 2
Characterization of the PAA-PAI properties with comparison to its corresponding to analogues.

Binder	Binding affinity			Electrode property		Slurry property
	Mechanical properties		Adhesion stress (mN mm^{-1})	Extension (μm)	Recovery (%)	Degree of phase separation (%)
	Ultimate strength (MPa)	Young's modulus (MPa)				
PAA	32.8	7.95	2.35	0.74	24.8	20.0
PAI	18.4	4.90	3.14	1.62	32.0	1.3
PAA-PAI	27.5	5.58	3.92	0.83	35.1	3.5

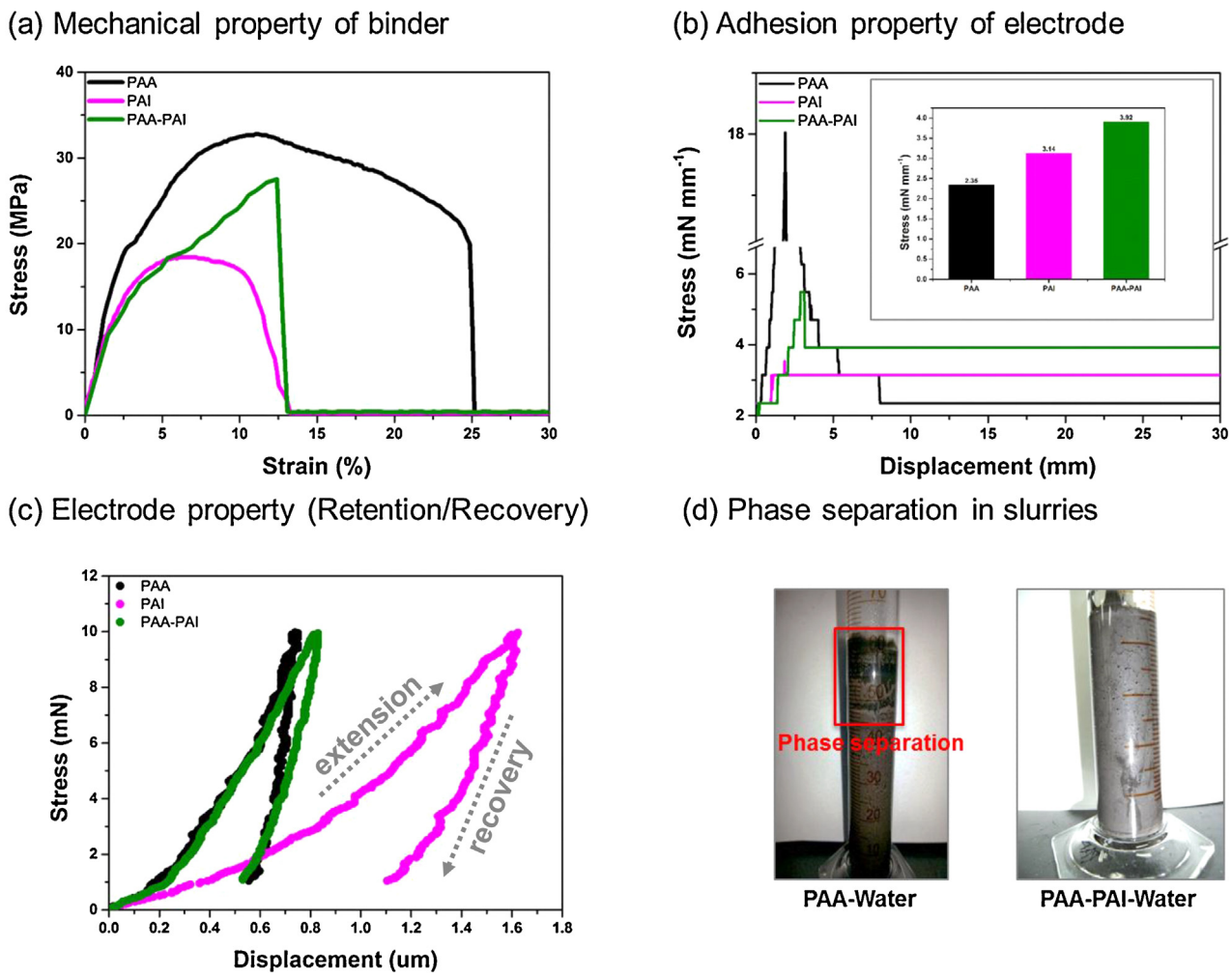

Fig. 6. Characterization of the PAA-PAI properties by binder screening method (a) Stress-strain curves for characterization of mechanical property in binder film, (b) adhesion property in electrode, (c) Degree of extension and recovery, (d) Analysis results for phase separation behavior.

372.3 mAh g^{-1} for PAA; 30.1%, 262.5 mAh g^{-1} for PAI). These results indicate that PAA–PAI was effective in facilitating higher utilization of the Si–graphite composite (better charge specific capacity) and enhancing cycle life (higher retentions). Because the specific capacity is directly proportional to the utilization of electrochemically active species and the degree of retention is significantly affected by electrode uniformity, it can be concluded that the well-balanced binder properties in PAA–PAI was beneficial in the suppression of undesired behavior (electrochemical grinding of active species and delamination from the Cu current collector), thus yielding a better

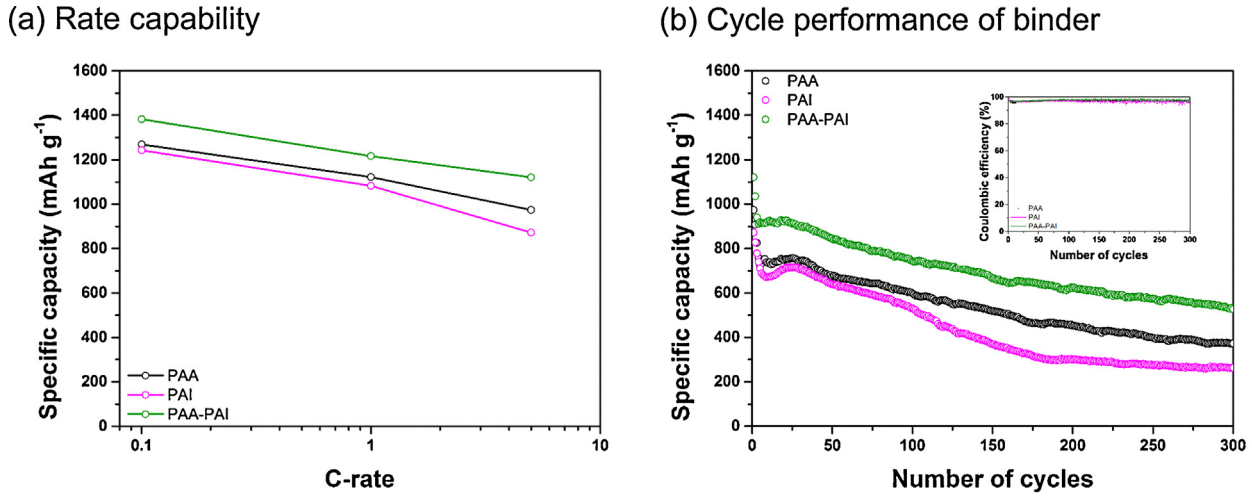

Fig. 7. (a) The results for rate capability, (b) Cycle performance of the PAA (black), PAI (pink) and PAA-PAI (green) at a rate of 5 C (inset: coulombic efficiency of the cell).

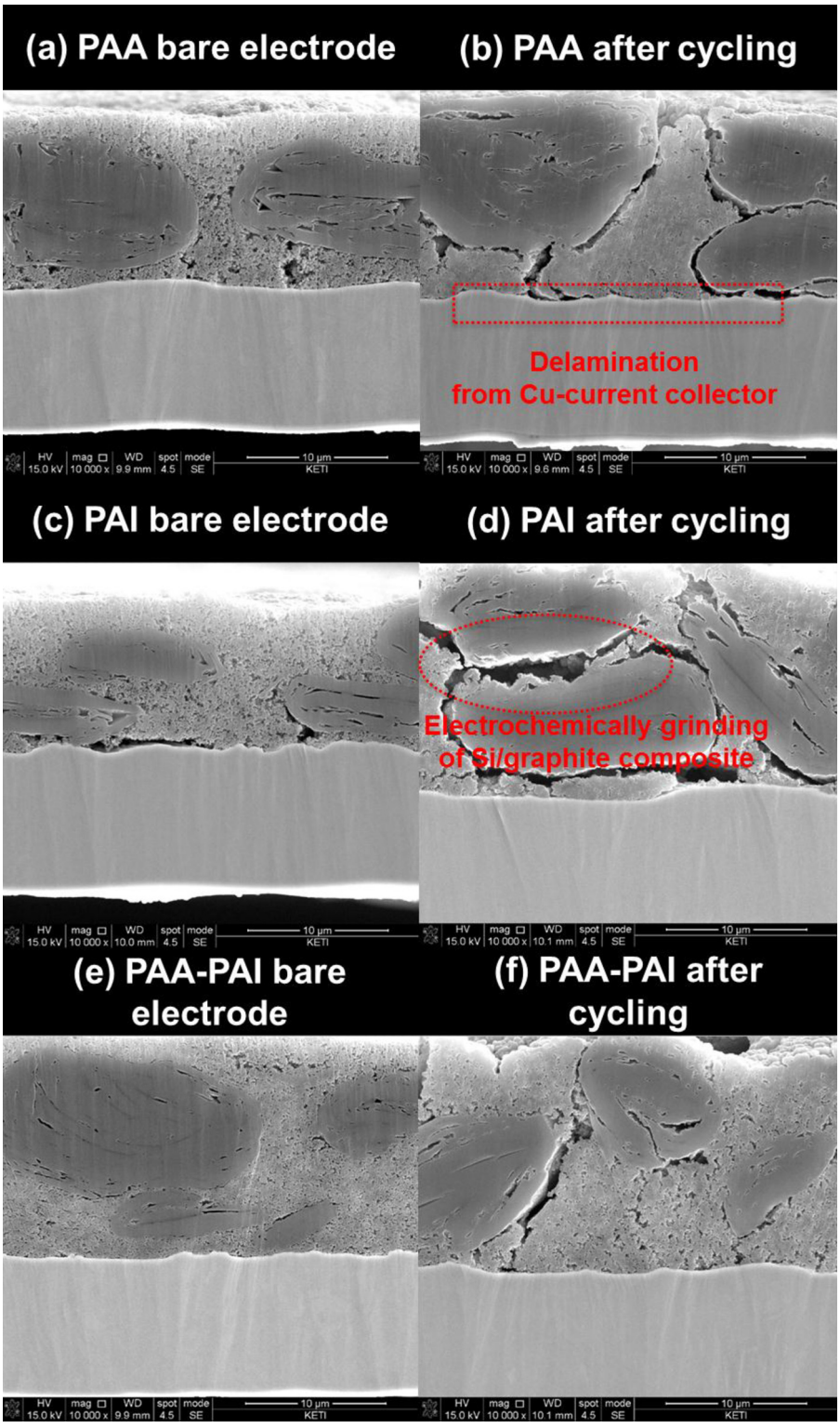

Fig. 8. Cross-sectional images of electrode (a) bare electrode with the PAA, (b) electrode with the PAA after 1 cycle, (c) bare electrode with the PAI, (d) electrode with the PAI after 1 cycle, (e) bare electrode with the PAA-PAI, (f) electrode with the PAA-PAI after 1 cycle.

electronic network in the Si–graphite electrode. The cross-sectional images of the cycled electrode (with each binder candidate) provided support for these explanations (Fig. 8). Images of the cycled electrodes with PAA and PAI indicate that delamination from the Cu current collector and electrochemical grinding of active material, respectively, occurred. On the other hand, the electrode cycled with PAA–PAI exhibited a more stable interface in terms of mechanical properties and adhesion affinity, where the materials appeared to cling together. In addition, PAA–PAI was more effective in preventing volume expansion of the Si–graphite composite: the cells consisting of PAA and PAI showed considerable amounts of volume expansion (20.4% and 51.7%, respectively) after 1 cycle, while the cell consisting of PAA–PAI exhibited a smaller volume expansion (13.8%) compared to its pristine electrode. These results clearly

indicate that the enhanced binder properties played an important role in the extent of active material utilization, resulting in better electrochemical performance of the Si–graphite anode.

4. Conclusions

Systematic characterization of binder properties was conducted to estimate the suitability of binder materials for a Si–graphite anode. An evaluation of four kinds of binders showed that PAA and PAI are recommendable candidates based on their unique properties (PAA: mechanical property and rigidity; PAI: adhesion affinity, recovery, and phase separation behavior). However, there were weaknesses that could hinder their successful utilization as the main binder: considerable amount of phase separation in PAA slurry and lower mechanical properties in PAI should be overcome to assure practical acceptance. In this respect, the co-polymerization approach offers an alternative means to modify binder properties by hybridization of PAA and PAI to offset their individual inferior properties and complement their individual superior properties. The characterization results showed that each weak point was completely compensated in the hybrid binder, leading to enhancement in overall properties. These enhancements were clearly reflected in the cycling performance, where the cell consisting of PAA–PAI exhibited remarkable specific capacity with excellent retention even after 300 cycles. Therefore, it can be concluded that fine tuning of the binder properties through an understanding of individual binders is an efficient approach to prevent deterioration of the Si–graphite composite. Insight gained from the characterization process will be helpful to further investigations of other binder candidates, which can lead to more efficient LIB systems.

Acknowledgement

This work was supported by the IT R&D program of MKE/KEIT (10044962, Development of polymeric binder for silicon-based anode).

References

[1] J.M. Tarascon, M. Armand, Issues and challenges facing rechargeable lithium batteries, Nature 414 (2001) 359.
[2] B. Scrosati, Recent advances in lithium ion battery materials, Electrochimica Acta 45 (2000) 2461.
[3] V. Etacheri, R. Marom, R. Elazari, G. Salitra, D. Aurbach, Challenges in the development of advanced Li-ion batteries: a review, Energy & Environmental Science 4 (2011) 3243.
[4] A.N. Jansen, A.J. Kahaian, K.D. Kepler, P.A. Nelson, K. Amine, D.W. Dees, D.R. Vissers, M.M. Thackeray, Development of a high-power lithium-ion battery, Journal of Power Sources 81–82 (1999) 902.
[5] B. Kennedy, D. Patterson, S. Camilleri, Use of lithium-ion batteries in electric vehicles, Journal of Power Sources 90 (2000) 156.
[6] M. Armand, J.M. Tarascon, Building better batteries, Nature 451 (2008) 652.
[7] J.O. Besenhard, J. Yang, M. Winter, Will advanced lithium-alloy anodes have a chance in lithium-ion batteries? Journal of Power Sources 68 (1997) 87.
[8] K. Kang, Y.S. Meng, J. Breger, C.P. Grey, G. Ceder, Electrodes with High Power and High Capacity for Rechargeable Lithium Batteries, Science 17 (2006) 977.
[9] C.K. Chan, H. Peng, G. Liu, K. McIlwrath, X.F. Zhang, R.A. Huggins, Y. Cui, High-performance lithium battery anodes using silicon nanowires, Nature Nanotechnology 3 (2008) 31.
[10] H. Li, X. Huang, L. Chen, Z. Wu, Y. Liang, A high capacity nano-Si composite anode material for lithium rechargeable batteries, Electrochemical Solid-State Letters 2 (1999) 547.
[11] A. Magasinski, P. Dixon, B. Hertzberg, A. Kvit, J. Ayala, G. Yushin, High-performance lithium-ion anodes using a hierarchical bottom-up approach, Nature Materials 9 (2010) 353.
[12] Z.S. Wen, J. Yang, B.F. Wang, K. Wang, Y. Liu, High capacity silicon/carbon composite anode materials for lithium ion batteries, Electrochemistry Communications 5 (2003) 165.
[13] M.N. Obrovac, L. Christensen, Structural changes in silicon anodes during lithium insertion/extraction, Electrochemical Solid-State Letters 7 (2004) A93.
[14] D. Larcher, S. Beattie, M. Morcrette, K. Edstrom, J.-C. Jumas, J.-M. Tarascon, Recent findings and prospects in the field of pure metals as negative electrodes for Li-ion batteries, Journal of Materials Chemistry 17 (2007) 3759.
[15] N.S. Hochgatterer, M.R. Schweiger, S. Koller, P.R. Raimann, T. Wöhrle, C. Wurm, M. Winter, Silicon/graphite composite electrodes for high-capacity anodes: influence of binder chemistry on cycling stability, Electrochemical Solid-State Letters 11 (2008) A76.
[16] S. Komaba, N. Yabuuchi, T. Ozeki, Z.-J. Han, K. Shimomura, H. Yui, Y. Katayama, T. Miura, Comparative study of sodium polyacrylate and poly(vinylidene fluoride) as binders for high capacity Si-graphite composite negative electrodes in Li-ion batteries, The Journal of Physical Chemistry C 116 (2012) 1380.
[17] R.R. Garsuch, D.-B. Le, A. Garsuch, J. Li, S. Wang, A. Farooq, J.R. Dahn, Studies of lithium-exchanged Nafion as an electrode binder for alloy negatives in lithium-ion batteries, Journal of The Electrochemical Society 155 (2008) A721.
[18] M.-H. Ryou, J. Kim, I. Lee, S. Kim, Y.K. Jeong, S. Hong, J.H. Ryu, T.-S. Kim, J.-K. Park, H. Lee, J.W. Choi, Mussel-inspired adhesive binders for high-performance silicon nanoparticle anodes in lithium-ion batteries, Advanced Materials 25 (2013) 1571.
[19] C.-H. Yim, F.M. Courtel, Y. Abu-Lebdeh, A high capacity silicon–graphite composite as anode for lithium-ion batteries using low content amorphous silicon and compatible binders, Journal of Material Chemistry A 1 (2013) 8234.
[20] N.-S. Choi, K.H. Yew, W.-U. Choi, S.-S. Kim, Enhanced electrochemical properties of a Si-based anode using an electrochemically active polyamide imide binder, Journal of Power Sources 177 (2008) 590.
[21] S.D. Beattie, D. Larcher, M. Morcrette, B. Simon, J.-M. Tarascon, Si electrodes for Li-ion batteries - a new way to look at an old problem, Journal of The Electrochemical Society 155 (2008) A158.
[22] D. Mazouzi, B. Lestriez, L. Roué, D. Guyomard, Silicon composite electrode with high capacity and long cycle life, Electrochemical Solid-State Letters 12 (2009) A215.
[23] A. Magasinski, B. Zdyrko, I. Kovalenko, B. Hertzberg, R. Burtovyy, C.F. Huebner, T.F. Fuller, I. Luzinov, G. Yushin, Toward Efficient Binders for Li-Ion Battery Si-Based Anodes: Polyacrylic Acid, ACS Applied Materials & Interfaces 2 (2010) 3004.
[24] Z.-J. Han, N. Yabuuchi, K. Shimomura, M. Murase, H. Yui, S. Komaba, High-capacity Si–graphite composite electrodes with a self-formed porous structure by a partially neutralized polyacrylate for Li-ion batteries, Energy & Environmental Science 5 (2012) 9014.
[25] X. Xiao, P. Liu, M.W. Verbrugge, H. Haftbaradaran, H. Gao, Improved cycling stability of silicon thin film electrodes through patterning for high energy density lithium batteries, Journal of Power Sources 196 (2011) 1409.
[26] J.-H. Kim, S.C. Woo, M.-S. Park, K.J. Kim, T. Yim, J.-S. Kim, Y.-J. Kim, Capacity fading mechanism of LiFePO4-based lithium secondary batteries for stationary energy storage, Journal of Power Sources 229 (2013) 190.
[27] B. Koo, H. Kim, Y. Cho, K.T. Lee, N.-S. Choi, J. Cho, A highly cross-linked polymeric binder for high-performance silicon negative electrodes in lithium Ion batteries, Angewandte Chemie International Edition 51 (2012) 1.
[28] K.-F. Arndt, A. Richter, S. Ludwig, J. Zimmermann, J. Kressler, D. Kuckling, H.-J. Adler, Poly(vinyl alcohol)/poly(acrylic acid) hydrogels: FT-IR spectroscopic characterization of crosslinking reaction and work at transition point, Acta Polymer 50 (1999) 383.
[29] E. Pretsch, P. Buhlmann, C. Affolter, Structure Determination of Organic Compounds, third ed., Springer-Verlag Berlin Heidelberg, New York, 2000.
[30] D.J. Pasto, C.R. Johnson, Organic Structure Determination, Prentice-Hall, Englewood Cliffs, New Jersey, 1969.